ELSEVIER

www.elsevier.nl/locate/jorganchem

Journal of Organometallic Chemistry 593–594 (2000) 307–314

Journal of Organometallic Chemistry

An experimental and theoretical study of the electronic and molecular structure of [Zn4(?4-S){μ-$S_2P(OC_2H_5)_2$}$_6$]: the first molecular model of ZnS

Alberto Albinati [a], Maurizio Casarin [b,*], Frank Eisentraeger [a,1], Chiara Maccato [b], Luciano Pandolfo [c,2], Andrea Vittadini [d]

[a] *Istituto di Chimica Farmaceutica e Tossicologica, Università di Milano, Milan, Italy*
[b] *Dipartimento di Chimica Inorganica, Metallorganica ed Analitica, Università di Padova, Padua, Italy*
[c] *Dipartimento di Chimica, Università della Basilicata, Potenza, Italy*
[d] *Centro di Studio sulla Stabilità e Reattività dei Composti di Coordinazione, C.N.R., Padua, Italy*

Received 10 June 1999; accepted 23 September 1999

Dedicated to Professor Fausto Calderazzo on the occasion of his 70th birthday.

Abstract

The electronic and molecular structure of hexakis[μ-(*O*,*O*′-diethyl dithiophosphate-S:S′)]-μ_4-thiotetrazinc, [Zn_4(μ_4-S){μ-$S_2P(OC_2H_5)_2$}$_6$] (**1**), has been investigated by combining X-ray diffraction measurements, UV–vis absorption spectroscopy and density functional calculations. The title compound is characterized by a Zn_4(μ_4-S)(μ-S_{12}) core consisting of a S atom at the center of a distorted tetrahedron of Zn ions, each of them placed at the center of an irregular tetrahedron of S atoms. Theoretical results point out that **1**, at variance to the isostructural [Zn_4(μ_4-S){μ-$S_2As(CH_3)_2$}$_6$] recently investigated by Albinati et al. [Inorg. Chem. 38 (1999) 1145], can be considered a well tailored molecular model of ZnS. Theoretical outcomes also indicate that the low energy region of the UV absorption spectrum of **1** includes transitions having a ligand-to-metal-charge transfer nature involving the excitation of an electron from the occupied μ_4-S 3p based atomic orbitals to the empty Zn 4s based levels.

Keywords: Zinc; Polynuclear zinc complexes; Molecular models; Clusters; Sulfides; X-ray structures

1. Introduction

In the recent past, nanometer-sized particles of semiconductors have been extensively investigated both experimentally and theoretically [1]. Indeed, when the diameter of a semiconductor crystallite is progressively decreased to the nanometer range, the spatial confinement of charge carriers produces substantial changes in the optical properties of the material (quantum size effect) [1]. A further reduction of the particle size yields clusters, which can be considered the smallest constituents, the molecular models [2], of a semiconductor. These clusters are particularly interesting to investigate because they provide insights into the properties of the solid and the opportunity of testing, also from an experimental point of view, the validity of the cluster approach [3] in studying localized phenomena in solids.

As a part of a systematic investigation of molecular models of oxides and sulfides [4], we recently reported an experimental and theoretical study of the electronic and molecular structure of two polynuclear complexes: [M_4(μ_4-S){μ-$S_2As(CH_3)_2$}$_6$] (M = Zn and Cd) [4d]. Both clusters are characterized by a M_4(μ_4-E)(μ-E_{12}) core very similar to that of [Zn_4(μ_4-O){μ-O_2CCH_3}$_6$] [4a] and [Zn_4(μ_4-O){μ-$O_2CN(C_2H_5)_2$}$_6$] [4b]; i.e. a chalcogenide E ion tetrahedrally coordinated to four metal ions, each of them placed at the center of a distorted

* Corresponding author. Tel.: +39-049-827-5164; fax: +39-049-827-5161.
E-mail address: casarin@chim01.unipd.it (M. Casarin)
[1] Permanent address: Organisch-Chemisches Institut, Universitaet Heidelberg, Heidelberg, Germany.
[2] Also corresponding author.

0022-328X/00/$ - see front matter
PII: S0022-328X(99)00552-5

tetrahedron of E ions. Casarin et al. [4a,b] have shown that both $[Zn_4(\mu_4\text{-}O)\{\mu\text{-}O_2CCH_3\}_6]$ and $[Zn_4(\mu_4\text{-}O)\{\mu\text{-}O_2CN(C_2H_5)_2\}_6]$ are well tailored molecular models of ZnO and $Zn_4O(BO_2)_6$ [5], while Albinati et al. [4d] pointed out very recently that, because of their electronic structure, $[M_4(\mu_4\text{-}S)\{\mu\text{-}S_2As(CH_3)_2\}_6]$ (M = Zn and Cd) clusters cannot be considered molecular models of the corresponding sulfides [6].

In the present paper, we present the results of an experimental and theoretical investigation of the electronic and molecular structure of $[Zn_4(\mu_4\text{-}S)\{\mu\text{-}S_2P(OC_2H_5)_2\}_6]$ (**1**) carried out by combining X-ray diffraction measurements [8], UV–vis absorption spectroscopy and density functional (DF) calculations. Our goal is that of looking into, and eventually tuning, the electronic properties of clusters containing a $Zn_4(\mu_4\text{-}E)(\mu\text{-}E_{12})$ core.

2. Experimental and computational details

2.1. Instrumentation, materials and synthesis

All reactions and manipulations were carried out under an atmosphere of dry argon with standard Schlenk techniques. Solvents were distilled under argon before use. ZnO (Prolabo) and *O*,*O*′-diethyl dithiophosphoric acid (90% Aldrich) were used without further purification. A Bruker SMART CCD diffractometer operating at 200 K was employed for the structural study. UV–vis absorption spectra were recorded on a Varian Cary 5E spectrophotometer and elemental analyses were provided by the Microanalysis Laboratory of the C.I.M.A. Department of the University of Padova.

2.2. Synthesis of $[Zn_4(\mu_4\text{-}S)\{\mu\text{-}S_2P(OC_2H_5)_2\}_6]$ (1)

Solid ZnO (6.7 g, 0.082 mol) was slowly added (1 h) to a vigorously stirred solution of *O*,*O*′-diethyl dithiophosphoric acid ($(C_2H_5O)_2P(S)SH$) (20 g 90% pure, 0.097 mol) in 15 ml of ethanol at 0°C. An exothermic reaction took place and the resulting white slurry was allowed to reach room temperature (r.t.) and further stirred for 24 h. The suspension was filtered off, the solid was thoroughly washed with ethanol and dried under vacuum, yielding 16 g of a white solid (**A**). Solid **A** was extracted with boiling ethanol to dissolve any possible bis(*O*,*O*′-diethyl dithiophosphate)zinc(II), $[Zn(\mu\text{-}S_2P(OC_2H_5)_2]_2$ [9], and the dried solid residue (**B**, 15 g) was extracted with boiling dichloromethane. The CH_2Cl_2 solution (about 100 ml) was concentrated under vacuum to about 10 ml; addition of 80 ml of ethanol caused the formation of a white precipitate ($[Zn_4(\mu_4\text{-}S)\{\mu\text{-}S_2P(OC_2H_5)_2\}_6]$, hereafter **1**, that was filtered, washed with ethanol and dried under vacuum. Yield 2.1 g (7.3% based on ZnO). Compound **1** was recrystallized from dichloromethane–ethanol. M.p.: 201–203°C. Elemental analysis: Calc. (found) for $C_{24}H_{60}O_{12}S_{13}P_6Zn_4$: C = 20.52 (20.45), H = 4.30 (4.05), S = 29.67 (30.25).

2.3. Structural study of $[Zn_4(\mu_4\text{-}S)\{\mu\text{-}S_2P(OC_2H_5)_2\}_6]$

Colourless crystals of **1**, suitable for X-ray diffraction measurements, were obtained by crystallization from dichloromethane–ethanol and are air stable. A prismatic single crystal was mounted for data collection on a glass fiber at a random orientation on a Bruker SMART CCD diffractometer operating at 200 K. The space group was determined from the systematic absences ($R3$ or $R\bar{3}$), while the cell constants were refined, at the end of the data collection, using 4260 reflections up to $\theta_{max} = 25^{\circ}$. Data were collected in the 'ω-scan mode' with steps of 0.3° with counting time for each 'frame' of 20 s.

The collected intensities were corrected for Lorentz and polarization factors [10], while an empirical absorption correction (based on the intensities of symmetry related reflections) was also applied using the SADABS program [11]. The standard deviations of intensities were calculated in terms of statistics alone, while those on F_o^2 were computed as shown in Table 1.

Selected crystallographic data are listed in Table 1 and in Table S1 of the supplementary material (see Section 5). Fractional coordinates and equivalent isotropic displacement parameters, a full listing of selected interatomic distances and angles, anisotropic thermal parameters and hydrogen coordinates are available as supplementary material.

The structure was solved by direct and Fourier methods using the SHELXS program [12] and refined in space group $R\bar{3}$ by full matrix least squares [12] by minimizing the function

$$\left[\sum w(F_o^2 - (1/k)F_c^2)^2\right]$$

Towards the end of the refinement, disorder of the 'POC_2H_5' fragments was apparent. Two positions were found for the oxygen atoms and included in the refinement (atoms O11a and O21a with partial occupancy of 0.3 and 0.2, respectively). The high value of the thermal factors also indicates positional disorder for the carbon atoms, but it was impossible to model it satisfactorily. The presence of the disorder is reflected in the lower accuracy of the bond distances in the $P(OC_2H_5)_2$ groups and the value of the R factors.

The refinement of the structure in the acentric group $R3$ did not resolve the disorder problem but gave a significantly higher R_w factor (0.19) [13]. For this reason, the centrosymmetric refinement, using less parameters, was retained. Anisotropic displacement parameters

were used for all atoms. The contribution of the hydrogen atoms, in their calculated position, was included in the refinement using a riding model ($U(H) = 1.5 \times U$(bonded atom) Å^2). No extinction correction was deemed necessary. Upon convergence the final Fourier difference map showed no significant peaks.

It should be noted that the solution obtained with this data set is different from that of Harrison et al. [9]. A refinement using their coordinates diverged with unrealistic temperature factors for some of the atoms and high residuals (> 25 e $\times$ Å^{-3}) in the Fourier difference maps. A possible explanation of this finding is that we have crystallized a different polymorph. In this regard it may be noted the significant change in the value of the cell constant c (even allowing for the difference in T) that may reflect differences between the two forms.

The scattering factors used, corrected for the real and imaginary parts of the anomalous dispersion, were taken from the literature [14]. All calculations were carried out by using the PC version of the SHELX-97 programs [12].

Table 1
Crystal and structure refinement data for **1**

Formula	$C_{24}H_{30}O_{12}P_6S_{13}Zn_4$
Molecular weight	1374.69
Temperature (K)	200
Diffractometer	Bruker SMART CCD
Crystal system	Trigonal
Space group	$R\bar{3}$
a (Å)	20.7147(2)
c (Å)	11.3972(2)
V (Å^3)	4235.32(9)
Z	3
$\rho_{calc.}$ (g cm^{-3})	1.62
μ (mm^{-1})	2.262
Radiation	Mo–K$_\alpha$ (graphite monochromated $\lambda = 0.71079$ Å)
Measured reflections	$\pm h$, $\pm k$, $\pm l$
θ Range (°)	$1.97 < \theta < 25.54$
No. data collected	10616
No. independent data	1664
No. observed reflections (n_o)	1197 [$\lvert F_o \rvert > 4.0\sigma(\lvert F \rvert)$]
Transmission coefficient	0.756–0.935
No. of paramaters refined (n_v)	99
R_{av} [a]	0.047
R, R_w^2 (obs, reflections) [b]	0.063, 0.168
R, R_w^2 (all data) [b]	0.097, 0.193
GOF [c]	1.111

[a] $R_{av} = \Sigma \lvert F_o^2 - F_{o,av}^2 \rvert / \Sigma_i \lvert F_o^2 \rvert$; $R = \Sigma(\lvert F_o - (1/k)F_c \rvert)/\Sigma \lvert F_o \rvert$.
[b] $R_w^2 = [\Sigma\, w(F_o^2 - (1/k)F_c^2)^2 / \Sigma\, w \lvert F_o^2 \rvert^2]$; where $w = [\sigma^2(F_o^2) + (0.0763P)^2 + 54.4099P]^{-1}$ and $P = \{[F_o^2 + \max(F_o^2)]/3.0\}$.
[c] GOF: $[\Sigma_w(F_o^2 - (1/k)F_c^2)^2/(n_o - n_v)]^{1/2}$.

2.4. Absorption spectra

The r.t. absorption spectrum of **1** was recorded in the 200–500 nm region by using a Varian Cary 5E spectrophotometer with a spectral bandwidth of 1 nm. A solution 5×10^{-3} M of **1**, obtained by dissolving the title compound in spectral grade CH_2Cl_2, was employed immediately after its preparation.

2.5. Theoretical study of $[Zn_4(\mu_4\text{-}S)\{\mu\text{-}S_2P(OC_2H_5)_2\}_6]$

All the calculations have been run by using the DMol code [15]. This is a DF numerical method where the Kohn–Sham equations are solved for systems with a finite size providing eigenvalues, eigenvectors and charge distribution by using numeric atomic orbital (NAO) basis sets. The following NAOs have been employed throughout the calculations. (a) Zn: the 1s–4s NAOs of the neutral Zn atom, the 3d–4p NAOs of Zn^{2+}. (b) S: the 1s–3p NAOs of the neutral S atom, the 3s–3d NAOs of S^{2+}. (c) P: the 1s–3p NAOs of the neutral P atom, the 3s–3d NAOs of P^{2+}. (d) O: the 1s–2p NAOs of the neutral O atom and the 2s–2p NAOs of O^{2+} and two sets of 1s, 2p and 3d NAOs generated from two hydrogenic calculations using $Z = 5$ and $Z = 7$. (e) C: the 1s–2p NAOs of the neutral C atom, the 2s–2p NAOs of C^{2+} and two sets of 1s, 2p and 3d NAOs generated from two hydrogenic calculations using $Z = 5$ and $Z = 7$. (f) H: the 1s NAO of the neutral H atom and two sets of 1s and 2p NAOs generated from two hydrogenic calculations using $Z = 1.3$ and $Z = 4$. The Zn 1s–2p and the S, P, O and C 1s NAOs have been kept frozen throughout the calculations in a fully occupied configuration, allowing their exclusion from the variational space. As far as the l value of the one-center expansion of the Coulomb potential about each nucleus is concerned, a value of l one greater than that in the atomic basis set has been found to provide sufficient precision [16]. In the present study we used the following degree of angular truncation: $l = 3$ for Zn and $l = 2$ for S, P, O, C and H. Eigenvalues were plotted as density of states (hereafter DOS) by using a 0.3 eV Lorentzian broadening factor. These plots, based on the Mulliken's prescription for partitioning the overlap density [17], have the advantage of providing information about the atomic composition of molecular orbitals (MOs) over a broad range of energy. Even though uniquely defined, the Mulliken's population analysis is rather arbitrary; nevertheless, it results very useful to gain a qualitative idea of the electron localization. In selected cases, MO plots have been used to assign the bonding character of corresponding orbitals. Finally, the μ-$S_2P(OC_2H_5)_2$ moieties have been replaced by μ-$S_2P(OCH_3)_2$. Throughout the paper we will refer to the $[Zn_4(\mu_4\text{-}S)\{\mu\text{-}S_2P(OCH_3)_2\}_6]$ model compound as $\mathbf{1}^{Me}$.

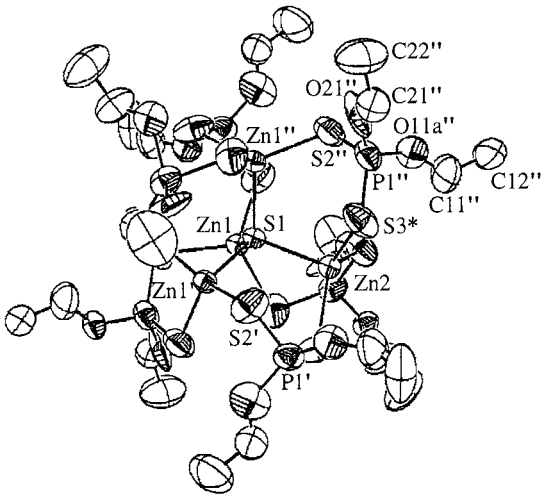

Fig. 1. ORTEP plots of $[Zn_4(\mu_4\text{-}S)\{\mu\text{-}S_2P(OC_2H_5)_2\}_6]$. Primed atoms are obtained by those umprimed through the following symmetry operations: $-y, x-y, z; -x+y, -x, z; x-y, x, -z$. Starred atoms are obtained from those umprimed by the following symmetry operations: $-x, -y, -z; y, -x+y, -z$.

Table 2
Selected bond lengths (Å) and angles (°) for **1**

Bond angles			
Zn1–S1	2.254(2)	P1–S2	1.930(4)
Zn1–S2	2.411(4)	P1–S3**	1.946(4)
Zn1–S2**[a]	2.404(3)	P1–O11	1.557(8)
Zn1–S2'''	2.411(3)	P1–O11a[c]	1.778(2)
Zn1–S3	2.479(4)	P1–O21	1.614(11)
Zn2–S1	2.347(3)	P1–O21a[c]	1.50(4)
Zn2–S3**[a]	2.403(3)		
Bond angles			
Zn1**–S1–Zn1*[a]	111.29(4)	S1–Zn2–S3*[a]	102.7(1)
Zn1–S1–Zn2	107.58(4)	S3*–Zn2–S3'''[b]	115.30(8)
Zn1–S1–Zn1'[b]	68.71(4)	Zn1–S2–P1	100.0(2)
Zn1**–S1–Zn2	72.48(4)	Zn1–S3–P1'''[b]	102.6(2)
S1–Zn1–S2	106.5(1)	Zn1–S2**–P1**[a]	108.3(2)
S1–Zn1–S3	103.1(1)	Zn2–S3''–P1''[b]	107.0(1)
S2–Zn1–S3	112.4(1)	S2–P1–S3**[a]	122.8(2)
S2–Zn1–S2**[a]	106.7(1)	S3–P1'''–S2'''[b]	122.8(2)
S3–Zn1–S2**[a]	110.6(1)		

[a] The starred (double starred) atoms are generated, from those in the asymmetric unit, by the symmetry operations: $-y, x-y, z; x-y, x, -z$, respectively.

[b] The primed atoms are generated from those unprimed by the symmetry operations: $-y, x-y, z; y, -x+y, -z; -x+y, -x, z$, respectively.

[c] O11a and O21a are the disordered oxygen atoms (see text).

3. Results and discussion

3.1. Crystal structure of $[Zn_4(\mu_4\text{-}S)\{\mu\text{-}S_2P(OC_2H_5)_2\}_6]$

The structure comprises independent $[Zn_4(\mu_4\text{-}S)\{\mu\text{-}S_2P(OC_2H_5)_2\}_6]$ molecules (see Fig. 1) held together by normal van der Waals contacts. Each molecule possesses a crystallographic symmetry with the S1 atom lying on a $-\bar{3}$ axis. As a result of the symmetry eight Zn atoms are generated and two Zn tetrahedra (each of them with a 50% occupancy) surround the central sulfur atom S1 (see Fig. 2(a), where a noticeable trigonal distortion is evident).

A selection of bond distances and bond angles of **1** is listed in Table 2, while an ORTEP view of its inorganic core is reported in Fig. 2(b). At variance to the structure published by Harrison et al. [9], our data indicates that the coordination of the μ_4-S atom (S1 in Figs. 1 and 2) consists of a distorted tetrahedron of Zn atoms with two different Zn–S separations (see Table 2) whose values may be compared with the average value of 2.265(6) Å reported in Ref. [9]. Moreover, the coordination of the two diethyl dithioposphate ligands is slightly asymmetric, as can be deduced by the Zn–S2 (av. 2.407(3) Å) and Zn–S3 (2.479(4) Å) bond distances. At variance to that, bond lengths and bond angles of the dithioposphate ligand are comparable to those previously reported [9].

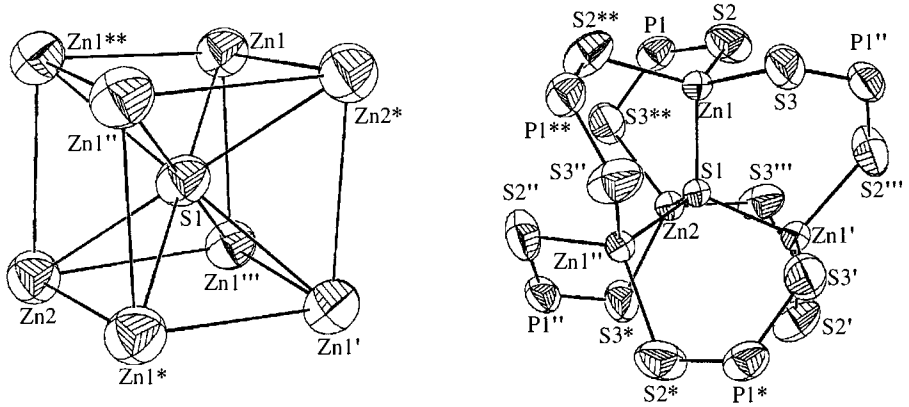

Fig. 2. (a) ORTEP plot of the coordination around the central S1 atom of $[Zn_4(\mu_4\text{-}S)\{\mu\text{-}S_2P(OC_2H_5)_2\}_6]$. (b) ORTEP plot of the inorganic core of **1** $[Zn_4(\mu_4\text{-}S)\{\mu\text{-}S_2P(OC_2H_5)_2\}_6]$.

3.2. Absorption spectroscopy measurements

The absorption spectrum of **1** between 220 and 350 nm, recorded immediately after its dissolution in spectral grade CH_2Cl_2, is shown in Fig. 3 together with the spectra of the solvent and $[Zn_4(\mu_4\text{-}S)\{\mu\text{-}S_2As(CH_3)_2\}_6]$ [4d]. The spectrum of the title compound consists of a strong absorption band centered at 228 nm (5.44 eV) with no shoulder on its low energy side. Interestingly, the energy position of this band perfectly agrees with the estimate reported by Blasse et al. [7] for the absorption maximum in the excitation spectrum of $Zn_4(\mu_4\text{–}S)^{6+}$ clusters encapsulated in a borate cage.

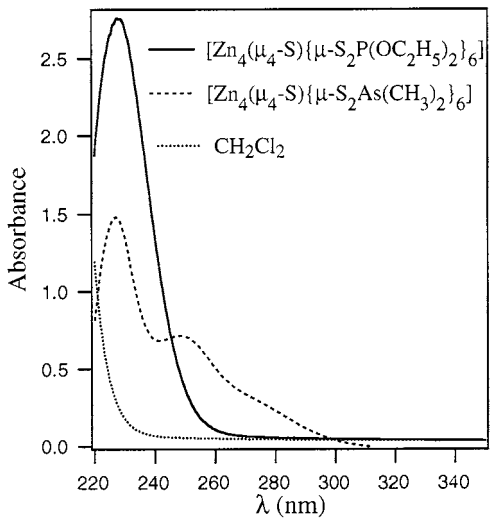

Fig. 3. UV absorption spectra of $[Zn_4(\mu_4\text{-}S)\{\mu\text{-}S_2P(OC_2H_5)_2\}_6]$ in CH_2Cl_2. For comparison the absorption spectra of $[Zn_4(\mu_4\text{-}S)\{\mu\text{-}S_2As(CH_3)_2\}_6]$ in CH_2Cl_2 and pure CH_2Cl_2 are also reported.

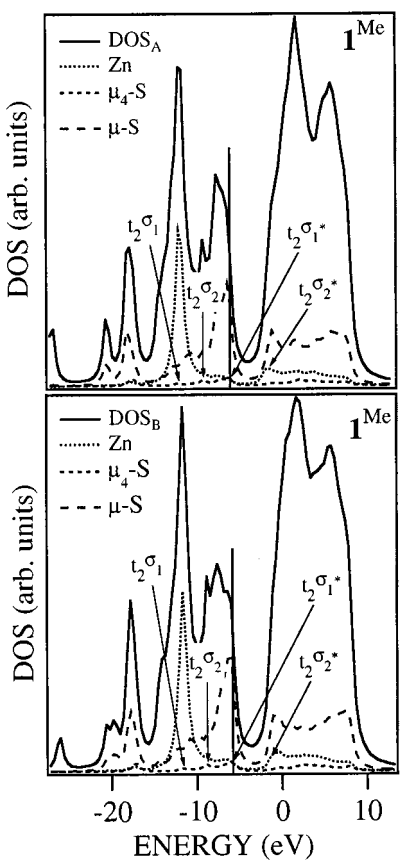

Fig. 4. Density of states (DOS) of $\mathbf{1}^{Me}$ computed with geometrical parameters herein reported (up) and with those of Ref. [9] (down). Partial DOS (PDOS) of Zn, μ_4-S, and μ-S are also displayed. The vertical bar represents the HOMO energy of $\mathbf{1}^{Me}$.

3.3. Theoretical results

Two sets of numerical experiments have been carried out: one by using geometrical parameters herein included, and another by employing the data of Harrison et al. [9]. The non-planar conformation of the $(\mu_4\text{-}S)Zn_2(\mu\text{-}S_2P)$ fragments (see Figs. 1 and 2(b)) allows an extensive mixing of the 'σ' and 'π' μ-S 3p AOs which prevents their factorization [18]. Moreover, the eigenvalue spectrum of $\mathbf{1}^{Me}$ is further complicated by the presence, in the same energy region, of the dithiophosphate O and μ-S non-bonding MOs. Thus, the analysis of the character of MOs is not straightforward, and the forthcoming discussion of the electronic structure of $\mathbf{1}^{Me}$ has been carried out by simply referring to DOS and PDOS curves.

The DOS of $\mathbf{1}^{Me}$ computed with geometrical parameters herein reported (DOS_A) and those of Ref. [9] (DOS_B) are displayed in Fig. 4 together with the PDOS of the $Zn_4(\mu_4\text{-}S)(\mu\text{-}S_{12})$ core constituents. DOS_A and DOS_B appear very similar, even though the $\Delta E_{(LUMO–HOMO)}$ [19] of the former (3.77 eV) is smaller than that of the latter (4.36 eV). We emphasize that the nature of frontier orbitals is however the same in both calculations.

The likeness between crystallographic data recorded at 200 K and at r.t. [9], the similarity between DOS_A and DOS_B, and the equivalence of the nature of frontier MOs indicate that the different $\Delta E_{(LUMO\text{-}HOMO)}$ in the two sets of calculations is due to the distortion of the $Zn_4(\mu_4\text{-}S)$ inner core revealed at 200 K [20]. The absence of such a distortion in the molecular structure determined at r.t. [9] prompted us to assume an analogous behavior in solution, and for this reason, the assignment of the UV absorption data will be carried out by referring to DOS_B.

In an ideal tetrahedral environment, the 3p AOs of the μ_4-S atom span the t_2 irreducible representation of the T_d point group [21]. The interaction of the occupied 3p μ_4-S AOs with empty t_2 Zn orbitals, e.g. linear combinations of Zn 4s and 4p AOs, only gives rise to occupied bonding combinations, while the interaction with filled t_2 Zn levels, e.g. linear combinations of Zn 3d AOs, produces occupied bonding and antibonding

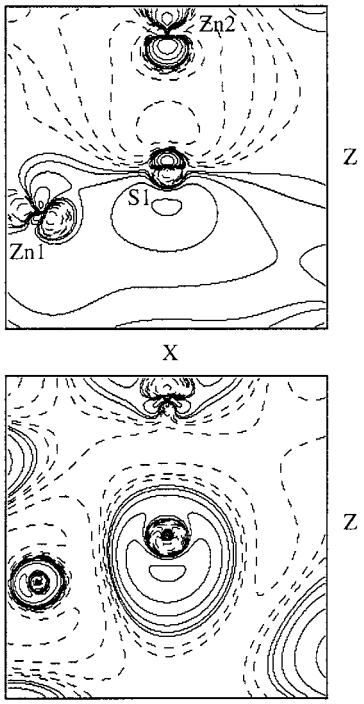

Fig. 5. Contour plots of a component of the $t_2^{\sigma_2}$ (up) and $t_2^{\sigma_2^*}$ (down) MOs. Contour values are ± 0.38, ± 0.20, ± 0.10, ± 0.025, ± 0.012, ± 0.006, ± 0.003 $Å^{1/2}$ $e^{-3/2}$ with negative values in dashed lines.

partners. Among the occupied levels, the μ_4-S 3p based AOs give rise to two peaks lying at ca. -9 and ca. -6 eV both in DOS_A and in DOS_B (see Fig. 4). The former peak includes MOs accounting for (μ_4-S)–Zn σ bonding (hereafter $t_2^{\sigma_2}$, see Fig. 5) between Zn empty orbitals and μ_4-S 3p based AOs, while under the latter are hidden the antibonding partners of the interaction between the Zn 3d and μ_4-S 3p AOs ($t_2^{\sigma_1^*}$, see Fig. 6) [22]. Interestingly, the $t_2^{\sigma_1^*}$ MOs are the HOMOs of $\mathbf{1}^{Me}$, and they have a strong participation (ca. 20%) in the μ_4-S 3p AOs [23]. As far as the unoccupied levels are concerned, those with a significant participation in the Zn 4s AOs [23] and accounting for a (μ_4-S)–Zn antibonding interaction ($t_2^{\sigma_2^*}$, see Fig. 5) are the LUMOs.

As a whole, theoretical outcomes, in agreement with results recently reported by Albinati et al. [4d], indicate that for $[Zn_4(\mu_4\text{-}S)\{\mu\text{-}S_2As(CH_3)_2\}_6]$, the lowering of symmetry around the μ_4-S atom has only a minor effect on the energy level degeneracies of the $Zn_4(\mu_4\text{-}S)$ inner core. Furthermore, the title compound fits both structural and electronic demands to be considered a molecular model [2] of ZnS.

Undoubtedly, the substitution of the $As(CH_3)_2$ fragments with the $P(OCH_3)_2$ ones causes important changes in the electronic structure of the $Zn_4(\mu_4\text{-}S)(\mu\text{-}S_{12})$ core. A better understanding of these changes can be gained by referring to Fig. 7, where the PDOS of the $Zn_4(\mu_4\text{-}S)(\mu\text{-}S_{12})$ constituents of $\mathbf{1}^{Me}$ and $[Zn_4(\mu_4\text{-}S)\{\mu\text{-}S_2As(CH_3)_2\}_6]$ are compared [24]. It is clear that, on passing from $[Zn_4(\mu_4\text{-}S)\{\mu\text{-}S_2As(CH_3)_2\}_6]$ to $\mathbf{1}^{Me}$, the μ-S 3p levels are uniformly stabilized by ca. 0.4 eV. This is consistent with a higher electron accepting capability of the $P(OCH_3)_2$ groups compared to the $As(CH_3)_2$ ones, and thus, the gross atomic charge of the μ-S atoms in $[Zn_4(\mu_4\text{-}S)\{\mu\text{-}S_2As(CH_3)_2\}_6]$ is computed to be more negative than in $\mathbf{1}^{Me}$ (-0.39 and -0.36 [25], respectively).

Interestingly, the HOMO of the arsenic derivative in its actual C_3 symmetry has a significant localization on the μ_4-S atom (see Fig. 7). Nevertheless, in agreement with data reported by Albinati et al. [4d], $[Zn_4(\mu_4\text{-}S)\{\mu\text{-}S_2As(CH_3)_2\}_6]$ cannot be considered a molecular model of ZnS because the lowermost unoccupied MOs are strongly concentrated on the peripheral μ-S atoms with a negligible participation of the Zn 4s levels.

Moving to the assignment of the UV absorption spectrum, we first point out the significant difference between the spectra of **1** and $[Zn_4(\mu_4\text{-}S)\{\mu\text{-}S_2As(CH_3)_2\}_6]$, both reported in Fig. 3. In particular,

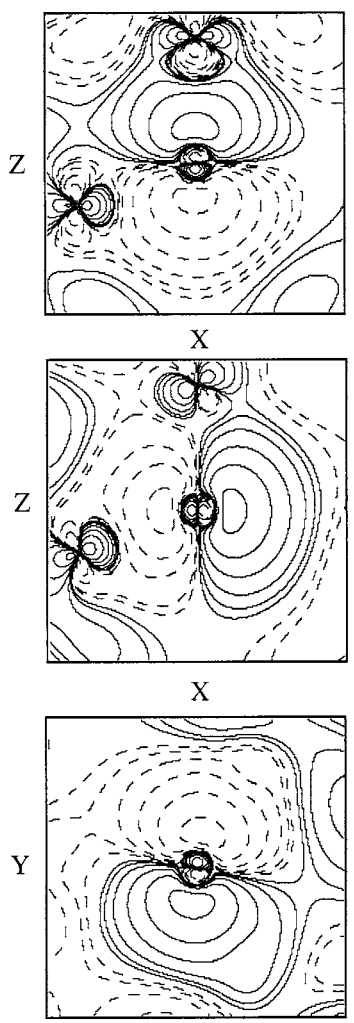

Fig. 6. Contour plot of the $t_2^{\sigma_1^*}$ MOs. Contour values are the same as in Fig. 5.

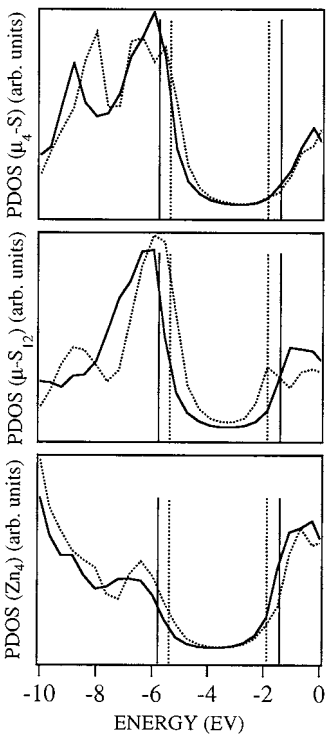

Fig. 7. Comparison of the (μ_4-S), Zn_4 and (μ-S_{12}) $PDOS_B$ for **1** (solid line) and $[Zn_4(\mu_4\text{-}S)\{\mu\text{-}S_2As(CH_3)_2\}_6]$ (dotted line). Vertical bars represent the HOMO and LUMO energies.

no absorption at $\lambda > 260$ nm (4.77 eV) is present in the spectrum of **1**. This has to be ascribed to two concomitant effects: (i) the LUMO–HOMO ΔE is larger in $\mathbf{1}^{Me}$ than in $[Zn_4(\mu_4\text{-}S)\{\mu\text{-}S_2As(CH_3)_2\}_6]$ (see Fig. 7); and (ii) the different composition of the frontier orbitals of the two compounds [26]. In detail, the low energy region of the UV absorption spectrum of **1** includes LMCT transitions corresponding to a $t_2^{\sigma 1*} \rightarrow t_2^{\sigma 2*}$ excitation, while at higher energies (lower wavelengths) transitions localized in the $S\text{–}P(OC_2H_5)_2\text{–}S$ ligands are present. These last transitions imply the excitation of an electron from μ-S lone pairs to MOs delocalized over the $(\mu_4\text{-}S)Zn_2(\mu\text{-}S_2P)$ rings. Ground state eigenvalue differences indicate that LMCT transitions lie, in good agreement with UV absorption data, at ca. 263 nm (4.7 eV) (the edge of the absorption band is at 260 nm), while excitation energies corresponding to interligand transitions are at ca. 225 nm (5.5 eV).

4. Conclusions

In this contribution we have presented a theoretical and experimental study of the electronic and molecular structure of $[Zn_4(\mu_4\text{-}S)\{\mu\text{-}S_2P(OCH_3)_2\}_6]$. X-ray diffraction measurements show, at low temperature, a slight trigonal distortion of the $Zn_4(\mu_4\text{-}S)$ inner core, which disappears at r.t. The combined use of experimental and theoretical outcomes indicates $[Zn_4(\mu_4\text{-}S)\{\mu\text{-}S_2P(OCH_3)_2\}_6]$ as a well tailored molecular model of ZnS. The comparison with data pertaining to other polynuclear zinc complexes characterized by the same $M_4(\mu_4\text{-}E)(\mu\text{-}E_{12})$ core demonstrates that the electronic properties of this core can be tuned through a judicious choice of peripheral substituents. This can be exploited for future molecular engineering of new models of extended systems.

5. Supplementary material

Crystallographic data (excluding structure factors) for the structure reported in this paper have been deposited with the Cambridge Crystallographic Data Center as supplementary publication no. CCDC-134693. Copies of this information may be obtained free of charge from: The Director, CCDC, 12 Union Road, Cambridge, CB2 1EZ, UK (Fax: +44-1223-336-033; email: deposit@ccdc.cam.ac.uk or www: http://www.ccdc.cam.ac.uk). A table of F_o/F_c may be obtained from the authors upon request.

Acknowledgements

This work was partially supported by Progetto Finalizzato 'Materiali Speciali per Tecnologie Avanzate II' of the C.N.R. (Rome). Furthermore, A.A. and F.E. acknowledge financial support from the Vigoni program.

References

[1] (a) A. Henglein, Chem. Rev. 89 (1989) 1861. (b) Y. Wang, N. Herron, J. Phys. Chem. 95 (1991) 525. (c) H. Weller, Angew. Chem. Int. Ed. Engl. 32 (1993) 41. (d) A. Henglein, Ber. Bunsenges. Phys. Chem. 101 (1997) 1562.

[2] A molecular model of a solid is an existing molecule or ion having a local structural arrangement similar to that of the solid, and frontier orbitals reproducing the states close to the band gap of the extended material.

[3] R.P. Messmer, Top. Curr. Phys. 8 (1977) 215.

[4] (a) R. Bertoncello, M. Bettinelli, M. Casarin, A. Gulino, E. Tondello, A. Vittadini, Inorg. Chem. 31 (1992) 1558. (b) M. Casarin, E. Tondello, F. Calderazzo, A. Vittadini, M. Bettinelli, A. Gulino, J. Chem. Soc. Faraday Trans. 89 (1993) 4363. (c) R. Bertoncello, M. Bettinelli, M. Casarin, C. Maccato, L. Pandolfo, A. Vittadini, Inorg. Chem. 36 (1997) 4707. (d) A. Albinati, M. Casarin, C. Maccato, L. Pandolfo, A. Vittadini, Inorg. Chem. 38 (1999) 1145.

[5] All the B atoms of $Zn_4O(BO_2)_6$ have a four-fold coordination. Tetrahedral BO_4 groups at the vertices of a truncated octahedra framework form a three-dimensional anion characterized by the presence of cubo-octahedral cavities encapsulating $Zn_4(\mu_4\text{-}O)$ clusters.

[6] Even though neither $[Zn_4(\mu_4\text{-}S)\{\mu\text{-}S_2As(CH_3)_2\}_6]$ nor $[Cd_4(\mu_4\text{-}S)\{\mu\text{-}S_2As(CH_3)_2\}_6]$ can be considered molecular models of ZnS

and CdS, respectively [4d], ligand-to-metal-charge-transfer (LMCT) transitions localized in their $M_4(\mu_4\text{-}S)$ inner core reproduce very well, both in nature and in energy, the maximum absorption of $Zn_4(\mu_4\text{-}S)^{6+}$ and $Cd_4(\mu_4\text{-}S)^{6+}$ clusters encapsulated in borate and aluminate cages, respectively [7].

[7] G. Blasse, G.J. Dirksen, M.E. Brenchley, M.T. Weller, Chem. Phys. Lett. 234 (1995) 177.

[8] The X-ray structure at room temperature (r.t.) of **1** has already been reported by Harrison et al. [9]. The present structural study, urged by the advises of a referee, was performed at 200 K.

[9] P.G. Harrison, M.J. Begley, T. Kikabhai, F. Killer, J. Chem. Soc. Dalton Trans. (1986) 925.

[10] SAINT: SAX Area Detector Integration: Siemens Analytical Instrumentation, 1996.

[11] G.M. Sheldrick, SADABS, Universität of Göttingen, Göttingen, Germany, in press.

[12] G.M. Sheldrick, SHELX-97, Structure solution and refinement package, Universität of Göttingen, Göttingen, Germany, 1997.

[13] W.C. Hamilton, Acta Crystallogr. 17 (1965) 502.

[14] A.J.C. Wilson (Ed.), International Tables for X-ray Crystallography, vol. C, Kluwer Academic, Dordrecht, The Netherlands, 1992.

[15] Dmol 2.2, Biosym Technologies, San Diego, CA, 1992.

[16] (a) B. Delley, J. Chem. Phys. 92 (1990) 508. (b) B. Delley, J. Chem. Phys. 94 (1991) 7245.

[17] R.S. Mulliken, J. Chem. Phys. 23 (1955) 1833.

[18] The 'σ' and 'π' character of linear combinations of μ-S 3p AOs was defined in Ref. [4d] with respect to the $(\mu_4\text{–}S)Zn_2(\mu\text{-}S_2As)$ ring planes.

[19] The acronyms LUMO and HOMO stand for lowest unoccupied MO and highest occupied MO, respectively.

[20] The lengthening of the Zn2–S1 bond lowers the energy of the empty MO accounting for the Zn2–S1 antibonding interaction.

[21] B.E. Douglas, C.A. Hollingsworth, Symmetry in Bonding and Spectra, Academic Press, London, UK, 1985.

[22] Bonding components ($t_2^{\sigma_1}$ MOs) of the interaction between Zn 3d and μ_4-S 3p AOs are also displayed in Fig. 4.

[23] Our attention is always concentrated on μ_4-S and Zn atoms because their tetrahedral coordination makes them quite similar to the sulphide and Zn(II) ions of ZnS.

[24] The (μ_4-S), Zn_4 and (μ-S_{12}) PDOS of $[Zn_4(\mu_4\text{-}S)\{\mu\text{-}S_2As(CH_3)_2\}_6]$ have been obtained for the actual C_3 structure [4d] rather than for the idealized C_{3v} one. Basis sets employed for these numerical experiments are the same of Ref. [4d].

[25] The charge of the μ-S atoms in $\mathbf{1}^{Me}$ is the same for both sets of coordinates.

[26] Both in $\mathbf{1}^{Me}$ and $[Zn_4(\mu_4\text{-}S)\{\mu\text{-}S_2As(CH_3)_2\}_6]$ μ_4-S 3p AOs significantly participate in the HOMOs, while the LUMOs have a completely different localization.